Journal of Hazardous Materials 192 (2011) 940–948

Contents lists available at ScienceDirect

Journal of Hazardous Materials

journal homepage: www.elsevier.com/locate/jhazmat

Large eddy simulation of pollutant gas dispersion with buoyancy ejected from building into an urban street canyon

L.H. Hu[a,*], Y. Xu[a], W. Zhu[b], L. Wu[a], F. Tang[a], K.H. Lu[a]

[a] State Key Laboratory of Fire Science, University of Science and Technology of China, Hefei, Anhui China
[b] Beijing Research Center of Urban System Engineering, Beijing, China

ARTICLE INFO

Article history:
Received 9 August 2010
Received in revised form
14 December 2010
Accepted 15 December 2010
Available online 21 December 2010

Keywords:
Street canyon
Large eddy simulation
Combustion pollutant
Building fire explosion
Critical re-entrainment velocity
Froude number

ABSTRACT

The dispersion of buoyancy driven smoke soot and carbon monoxide (CO) gas, which was ejected out from side building into an urban street canyon with aspect ratio of 1 was investigated by large eddy simulation (LES) under a perpendicular wind flow. Strong buoyancy effect, which has not been revealed before, on such pollution dispersion in the street canyon was studied. The buoyancy release rate was 5 MW. The wind speed concerned ranged from 1 to 7.5 m/s. The characteristics of flow pattern, distribution of smoke soot and temperature, CO concentration were revealed by the LES simulation. Dimensionless Froude number (Fr) was firstly introduced here to characterize the pollutant dispersion with buoyancy effect counteracting the wind. It was found that the flow pattern can be well categorized into three regimes. A regular characteristic large vortex was shown for the CO concentration contour when the wind velocity was higher than the critical re-entrainment value. A new formula was theoretically developed to show quantitatively that the critical re-entrainment wind velocities, u_c, for buoyancy source at different floors, were proportional to $-1/3$ power of the characteristic height. LES simulation results agreed well with theoretical analysis. The critical Froude number was found to be constant of 0.7.

1. Introduction

With the fast development of the urban society, more and more high and ultra high-rise buildings have been constructed one after another in the metropolises. These high and ultra high-rise buildings are usually built along the two sides of the roads or business streets. They compose so-called "urban street canyon" as defined by Vardoulakis et al. [1] as "a street with buildings lined up continuously along both sides". Street canyon is an important element in modern cities. Now, it is an important concern of the risk assessment for accidents involving accidental hazardous materials releases, especially pollutant gases, in urban areas. These pollutions will pose a great hazard to both human health and the environmental safety with the aid of the wind. So, in recent years, many studies have been carried out on pollutant dispersion in and above the urban street canyons.

Previous studies e.g., [2–15] had provided valuable contributions to the reveal of the flow patterns and behaviors, as well as their influence on the dispersion of pollutants in a street canyon. Such flow behaviors and dispersion characteristics included wakes, stagnating zones, recirculation vortex under a wind flow with the obstruction of a street canyon. The pollutants considered in these previous studies, both solid soot and gaseous species, included that released from the industry, the vehicle engine and the accidental spills of hazardous materials. However, no matter what kind of contamination sources were concerned, the buoyancy effect was rarely considered in above studies. Although several researchers [16–20] have investigated buoyancy effects on flow and pollutant dispersion in street canyons, those works deal with the scenario of ground or building wall heating by sunlight. For example, the flow characteristics within street canyons had been investigated by Kim and Baik [16,17] with bottom or roof heating, and by Panskus et al. [18] and Richards et al. [19] with building wall heating. Dimitrova et al. [20] had studied the thermal effects on the wind field characteristics within the urban environment. The temperature difference between the street bottom/building wall and the ambient air considered in these works were all less than 50 °C.

However, in the real world, fire combustion or explosion, as a strong self-standing buoyancy source with pollutant products, also exists and can yield large amount of harmful smoke soot and toxic gases, such as carbon monoxide (CO). These pollutants will also lead to adverse impacts on the urban air quality and inhabitants health [21,22]. Such accidents include the fire explosion of an oil tank, the spontaneous ignition fire of a vehicle, or a big building

* Corresponding author at: State Key Laboratory of Fire Science, University of Science and Technology of China, JinZhai Road, 96, Hefei, Anhui, 230026, China. Tel.: +86 551 3606446; fax: +86 551 3601669.
E-mail address: hlh@ustc.edu.cn (L.H. Hu).

0304-3894/$ – see front matter © 2010 Elsevier B.V. All rights reserved.
doi:10.1016/j.jhazmat.2010.12.063

Nomenclature

C_p	specific heat capacity (J kg^{-1} K^{-1})
Fr	Froude number
g	Acceleration of gravity (m/s^2)
$\dot{Q}$	Convective heat flow rate at the window (kW)
r_0	Equivalent radius of the heat source (m)
T_a	Ambient temperature (K)
u	Wind velocity (m/s)
Z	Characteristic height (m)
ΔT_Z	Mean temperature rise at location Z in the central axis (K)
Θ	Dimensionless temperature

Greek symbols

ρ_Z	Local density of the hot gases current (kg/m^3)

Subscripts

a	ambient
c	critical
Z	at characteristic height of Z

fire, in which the temperature difference between the buoyancy source and the ambient air will up to 500 °C or more to contribute a strong thermal effect. The current research of buoyancy effect on the transportation of these hazardous materials in urban elements is still very few. Complex interaction between the wind flow and the buoyant pollutant flow will come forth, along with the existence of a building obstacle. A recent study by Hu et al. [23] had investigated the flow pattern in urban street canyon in presence of strong buoyant contamination sources at the street floor center. A particular phenomenon was discovered that the initially buoyancy-driven rising pollutants would be re-entrained back and accumulated in the street canyon when the wind velocity is beyond a certain critical level. The concept of "critical re-entrainment wind velocity" was thus brought forward based on the phenomenon observed. This critical re-entrainment wind velocity, as an important parameter to be concerned, was found to increase asymptotically with the heat/buoyancy release rate of the contamination source.

However, there is another more realistic scenario, in which the fire or explosion, as a strong buoyancy source, is occurred in the building with dangerous smoke soot and gases ejected out from the broken building window, such as those in 911 catastrophe of World Trade Center collapse caused by the fire explosion and in many other high-rise building fires, into the urban street canyon. Under such a scenario, a spill gas plume is formed and attached to the external building wall, which differs definitely from a freely standing plume at the street floor center as shown in Fig. 1. For such a spill gas plume, the fresh air entrainment from the wall side is restrained. The entrainment mass flux of fresh air into the plume is much lower, thus the decrease of plume gas temperature and the dilution of pollutant concentration with height is slower, than that of a freely standing buoyant pollution plume. The transportation of the buoyancy should be also definitely different. Previous study by Hu et al. [24] in a road tunnel had shown that the temperature distribution and the critical longitudinal ventilation velocity to arrest the upwind buoyant gas dispersion with fire near the tunnel wall was different from that with fire at the tunnel center. For such a scenario with buoyancy-driven pollutants ejected out from the side building into the street canyon, one more parameter is coming forth when considering the critical re-entrainment wind velocity. That is the height from the floor where the buoyant contamination source is located to the top of the street canyon, as the fire or explosion can occur at different building floor levels. The pollution

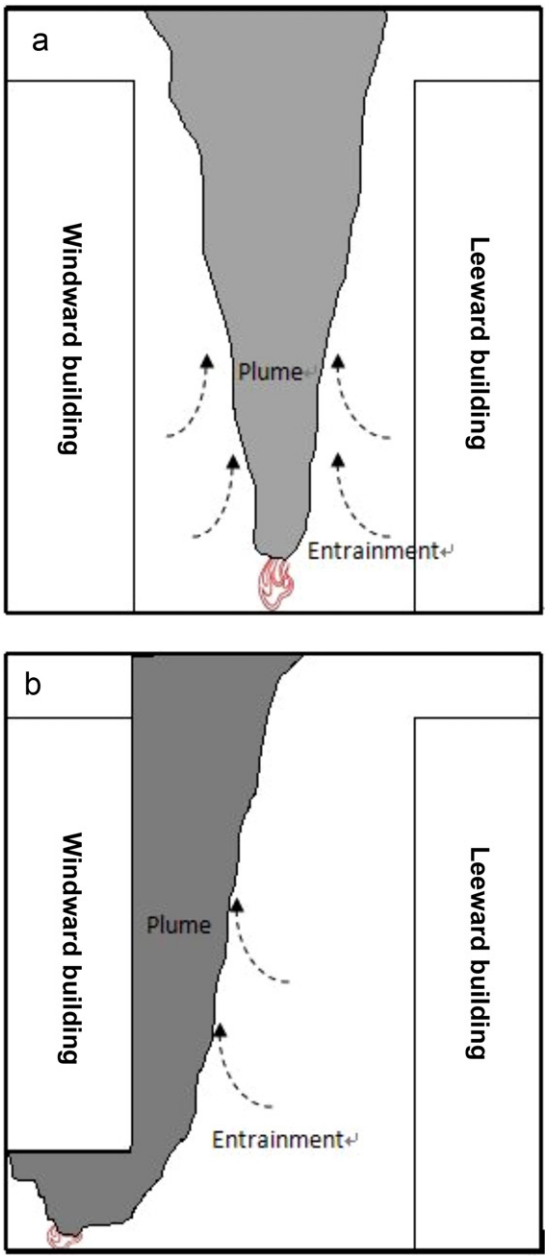

Fig. 1. Gas plumes for buoyant contamination source at street ground center and in the building of an urban street canyon.

plume temperature at the top of the street canyon should be higher with stronger buoyancy when the fire or explosion is occurred at higher floor levels. The critical re-entrainment wind velocity should be different from that with fire at the street floor center and needs to be further investigated.

In order to have an in-depth understanding of the flow pattern and pollutant dispersion in street canyon, three major research methods have been applied in the literatures: field measurements e.g., [2–5], physical modeling including wind tunnel experiments e.g., [6–9,18,19] and water tank experiments e.g., [10,11], and numerical simulations e.g., [12–17,20,23]. As the best method, field measurement is capable of getting the most realistic data, but also requires a lot of manpower and equipments at the same time. Although the physical modeling experiment is an available choice, such experimental researches on the flow pattern of street canyon coupled with a buoyancy source is still in its early stage and very few with a strong buoyancy effect. The knowledge to carry out such

physical modeling experiments is still lacking. Numerical simulation method is capable of making a good alternative for physical modeling. So far, large numbers of computational fluid dynamics (CFD) software have been developed. The most distinguishing feature of any CFD model is its treatment of turbulence. Three kinds of CFD turbulent models are popularly used: direct numerical simulation (DNS), Reynolds-averaged Navier–Stokes (RANS) $k-\varepsilon$ turbulence model and large eddy simulation (LES). DNS solves directly the Navier–Stokes equations without any turbulence model. The smallest dissipative scale, which is known as Kolmogorov scale, is resolved. So it can describe turbulence accurately. But DNS needs too many computer resources. On the other hand, RANS $k-\varepsilon$ turbulence model separates the flow variables into mean component and the fluctuating component (the so-called Reynolds decomposition). It does not solve the instantaneous Navier–Stokes equations. RANS $k-\varepsilon$ turbulence model is used to solve the time-averaged equations. It is clear that there is a fatal disadvantage in the RANS $k-\varepsilon$ turbulence model that it cannot predict the unsteadiness and intermittency of the turbulence flow accurately. So it is not very suitable to simulate the transient flow characters in and above the street canyon. As the compromise of the former two models, LES computes directly the large-scale eddies, and the sub-grid scale dissipative processes are simulated using sub-grid models (SGM). Most of all, LES can predict the unsteadiness and intermittency of the turbulence structure, which is the most important feature of a strong buoyancy-driven flow. In the guidelines described by Tominaga et al. [25] for practical applications of CFD to simulate pedestrian wind environment around buildings, which is proposed by the Working Group of the Architectural Institute of Japan (AIJ) as a good guide for important points when using RANS models, it is also deemed to be desirable to use a large eddy simulation (LES) model in order to obtain more accurate results. Therefore, large eddy simulation (LES) is chosen as the tool of this study to simulate the flow behavior and pollutant dispersion with buoyancy effect in and above the street canyon.

So in this article, the dispersion of buoyant pollutant smoke soot and gas ejected from a side building into a street canyon under a perpendicular wind flow is investigated by LES. The effect of the standing floor level of the buoyancy source is considered. One of the most important objectives of this study is to find out the relationship between the critical re-entrainment wind velocity and the characteristic height from the fire floor to the top of the street canyon. In LES simulations, the numerical method and model configurations are described. Pollutant dispersion flow pattern are investigated under different wind flow velocities. The smoke temperature and CO concentration distribution are computed. Theoretical analysis is then also carried out by introducing dimensionless parameter in turbulent buoyant flow dynamics theory, to consider the competition of buoyancy force of the ejected hot contamination flow with the inertial force of the wind flow at the top of the street canyon, and its effect on the dispersion of these hazardous products with strong buoyancy. Based on the LES simulations and theoretical analysis, the smoke soot field and flow pattern, as well as the temperature and CO concentration distribution in and above the street canyon are revealed. The theoretical deduced equation on variation law of the critical re-entrainment velocity with the characteristic height is finally compared with the LES simulation results.

2. Numerical method and model configuration

2.1. Numerical CFD methodology

Fire dynamics simulator (FDS) [26,27], as a computational fluid dynamics model for buoyancy-driven fluid flow, is used to investigate the dispersion characteristics for such a scenario. FDS is developed by National Institute of Standards and Technology (NIST) in co-operation with VTT Technical Research Centre of Finland, and others in the fire-safety community, as now a popular CFD tool in fire related researches, as well as used to simulate the concentration and flow distribution in urban street canyons (e.g., [28]). FDS solves the basic conservation of mass, momentum and energy equations for a thermally expandable, multi-component mixture of ideal gases [26,27]. A description of the model, many validation examples, and a bibliography of related articles and reports may be found on the web at http://fire.nist.gov/fds/. The core algorithm is an explicit predictor–corrector scheme, second order accurate in space and time [26,27]. It contains large eddy simulation (LES) and direct numerical simulation (DNS). In this study, LES is used to perform the calculation. The governing equations for LES simulation are as follows [27]:

Conservation of mass and transport for individual gaseous species, Y_α:

$$\frac{\partial}{\partial t}(\rho Y_\alpha) + \nabla \cdot \rho Y_\alpha \vec{u} = \nabla \cdot \rho D_\alpha \nabla Y_\alpha + \dot{m}'''_\alpha + \dot{m}'''_{b,\alpha} \quad (1)$$

where Y_α is the mass fraction of the individual gaseous species, $\dot{m}'''_{b,\alpha}$ is the production rate of species α by evaporating droplets/particles and $\dot{m}'''_\alpha$ is the mass production rate of species α per unit volume.

Conservation of momentum:

$$\frac{\partial}{\partial t}(\rho \vec{u}) + \nabla \cdot \rho \vec{u}\vec{u} + \nabla p = \rho g + \vec{f}_b + \nabla \cdot \tau_{ij} \quad (2)$$

Transport of sensible enthalpy, h_s:

$$\frac{\partial}{\partial t}(\rho h_s) + \nabla \cdot \rho h_s \vec{u} = \frac{Dp}{Dt} + \dot{q}''' - \dot{q}'''_b - \nabla \cdot \dot{\vec{q}}'' + \varepsilon \quad (3)$$

LES computes directly the large-scale eddies, and the sub-grid scale dissipative process is modeled using sub-grid models (SGM). The SMG and the choice of related parameters in SMG of FDS model were described in detail in the former study [23].

The convergence criteria in FDS model is not based on residue judgement, as used in many other CFD models, especially those based on RANS turbulence model. In FDS, the Courant–Friedrichs–Lewy (CFL) criterion [29,30] is used along with a self-varying time step [27] for justifying the computational convergence. The physical meaning of such a convergence criteria is that when computing a wave crossing a discrete grid, the time step must be less than the time for the wave to travel adjacent grid points. This criterion is more important for large-scale calculations where convective transport dominates the diffusive one. In FDS, the estimated velocities are tested at each time step to ensure that the following CFL criterion is satisfied [27]:

$$\delta t \cdot \max\left(\frac{|u_{ijk}|}{\delta x}, \frac{|v_{ijk}|}{\delta y}, \frac{|w_{ijk}|}{\delta z}\right) < 1 \quad (4)$$

During the calculation, the time step is varying and constrained by the convective and diffusive transport speeds to ensure that the CFL condition is satisfied at each time step [27]. The initial time step is set automatically in FDS by the size of a grid cell divided by the characteristic velocity of the flow. The default value of the initial time step is $5(\delta x \delta y \delta z)^{1/3}/\sqrt{gH}$, where δx, δy, and δz are the dimensions of the smallest grid cell, H is the height of the computational domain, and g is the acceleration due to gravity [27]. The time step will eventually get to be a quasi-steady value when the flow field reaches a quasi-steady state.

2.2. Physical model setup

The size of street canyon model used in this simulation was the same as the one used by Baker et al. [15] and Hu et al. [23], as shown in Fig. 2. A domain of 24 m wide, 40 m long and 40 m high

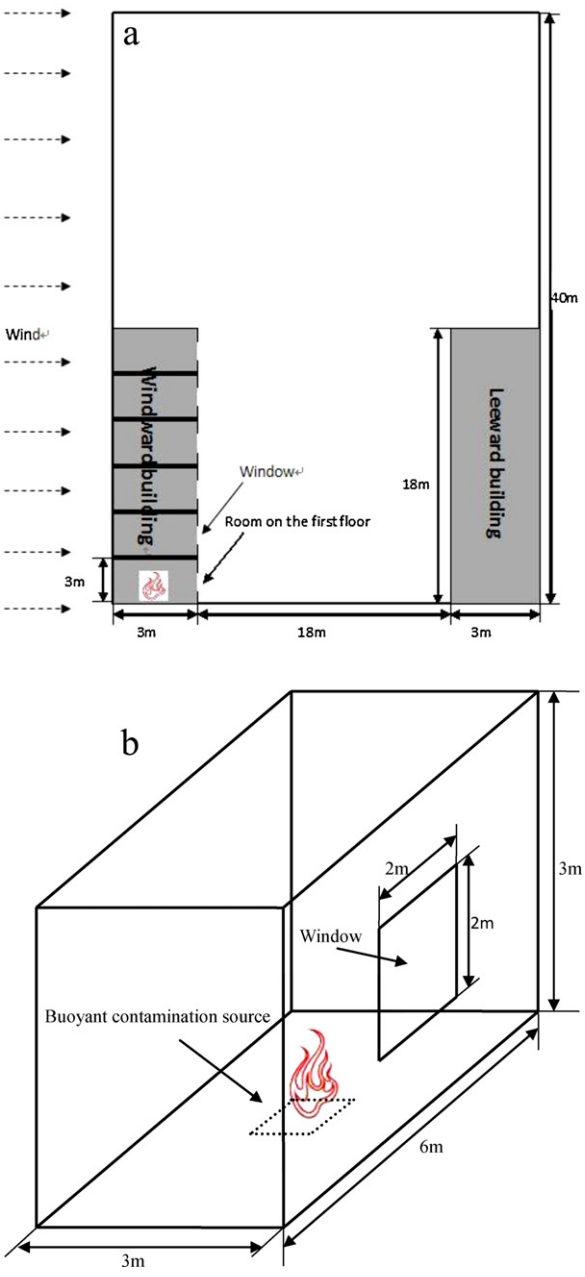

Fig. 2. Model configuration of the street canyon.

was built. Two buildings of 3 m wide, 40 m long and 18 m high were set at both sides of the domain to create an idealised street canyon of 18 m wide and 18 m high with an aspect ratio (W/H) of 1. In this simulation, a buoyancy source room (3 m × 6 m × 3 m) was also set in the windward building besides the street canyon. The buoyancy release rate of the source was 5 MW. The buoyancy source positions were considered at different floors, where the height of each storey was 3 m. Fig. 2(a) shows the case that the buoyant contamination source room is in the first floor. The buoyancy source room had a window of 2 m wide and 2 m high, which was in the middle of the wall facing street canyon. These windows at different floors were closed during the simulation, except for that of the buoyancy source room.

The wind flow was set to be perpendicular to the axis of the street canyon with different levels of velocities. Flow pattern and pollutant dispersion characteristics in and above the street canyon were investigated. The critical re-entrainment wind velocity was then found based on these characteristics. A uniform horizontal inlet flow was set to blow into the left side of the simulation domain, whose top and other three sides were all naturally opened [27] with no initial velocity boundary condition specified. The Reynolds number of the inlet flow, defined by $Re = uH/\nu$ where ν is the dynamic viscosity of air, was about ranged in $1.2–9 \times 10^6$ with wind velocity of 1–7.5 m/s. It was proved in literature [28], that for street canyon with $W/H = 1$, the FDS still predicted the measurements of flow velocity field in the wind tunnel experiments in good agreement with a uniform inflow boundary condition with no turbulence intensity specified. It was also concluded [31] that the turbulence level inside the canyon is not very sensitive to the external turbulence condition for such square canyon in the skimming flow regime, since the shear layer at the interface acts as a filter for the incoming turbulent structures. The wind velocity used for the simulations are summarized in Table 1. When the wind velocity is approaching the critical re-entrainment velocity, the incremental resolution of the wind velocity concerned in the simulation cases is controlled to be 0.1 m/s, which constrained the uncertainty of the critical re-entrainment wind velocity quantified by these simulations to be less than 0.1 m/s.

In LES simulation, the grid size is an important factor to be considered, which should be fine enough to include the turbulence scales associated with the largest eddy motions which can be described accurate enough by the SGM. Balance has to be considered for the gird size and the computation ability. Smaller gird size gives more detailed flow information but needs more computation resource. However, the basis of large eddy simulation is that accuracy increases as the numerical mesh is refined. Baker et al. [15] used, in his LES simulations for a street canyon with same configuration here, the grid size in the x- and y-direction of 0.3 m and 1.0 m, respectively. In the z-direction, the grid size was set to be 0.3 m in the street canyon and increased to be a maximum dimension of 5 m above the canyon. A smaller uniform gird system as that in the former study [23] was used here, which was uniform of 0.25 m in the three spatial directions. The cell number was $96 \times 160 \times 160$ in the x-, y- and z-direction respectively (total 2,457,600 cells).

Since there is still no such wind tunnel experimental data available for the scenario of this article with a strong buoyancy source, validation of the numerical model predictions had been considered separately from three aspects, the flow velocity field, the gas dispersion characteristics and the plume parameters under a wind condition. For the flow velocity field prediction, the numerical model had been validated [23] to be capable of well capture the flow dynamic characteristics within the street canyon. The wind tunnel experiment by Salizzoni et al. [31] was used to compare with FDS predictions with a uniform inlet wind flow boundary condition. The street canyon model in the wind tunnel experiment was

Table 1
Summary of simulation cases.

Floor level	Wind velocity													
1st floor	1	2	2.5	2.6	2.7	2.8	2.9	3	3.4	4	4.5	5	/	/
2nd floor	1	2	2.5	2.8	2.9	3	3.1	3.2	3.3	4.5	5	5.5	/	/
3rd floor	1	2	2.5	3	3.3	3.4	3.5	3.6	3.7	4	4.5	5	5.5	/
4th floor	1	2	2.5	3	3.3	3.5	3.7	3.8	3.9	4	4.1	5	5.5	5.8
5th floor	1	3	4	4.1	4.2	4.3	4.4	4.7	5	5.5	6	6.5	7	7.5

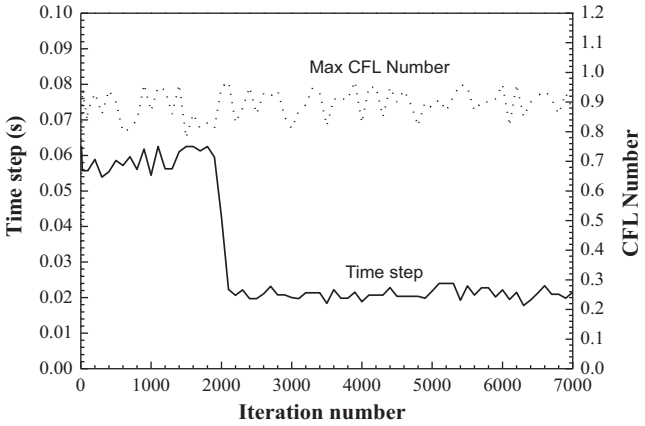

Fig. 3. Time step and CFL convergence of the simulation.

0.06 m wide and 0.06 m high, with a horizontal constant external wind flow of 6.8 m/s. The comparison of experimental data and FDS predictions, for the profiles of the mean horizontal velocity U as a function of height z at the mid-length of the canyon, and of the mean vertical velocity W as a function of x at the canyon mid-height were in good agreement [23]. More detailed information about the numerical scheme, the model setup and the validation can be found in the former report [23]. For the prediction of CO dispersion, the yield of the contamination, including the smoke soot and CO species was computed automatically by the sub-combustion model provided in FDS based on mixture fraction [23]. The FDS model had also been validated by full scale experiments [32] to be able to well predict the yield of CO species and their transportation by thermally driven flow with strong buoyancy. Chang [28] reported that the FDS LES agreed much better with the wind tunnel experimental results than those from FLUENT RANS $k-\varepsilon$ model in predicting the concentration and flow distribution in urban street canyons. For the prediction of buoyant plume parameters, validation work of FDS LES predictions for the development of large fire plume under the force of horizontal cross wind flow had also been formerly conducted by Hu et al. [33,34]. It was shown that the plume temperatures predicted by FDS LES were in good agreement with full scale experimental data in a real road tunnel.

A typical time-evolution of the time step and the corresponding maximum CFL number for the LES simulation in this article is shown in Fig. 3. The sudden drop of the time step value takes place when the fire starts. The strong buoyancy provided by the fire source will enhance the turbulence of the flow, thus it needs smaller time step to resolve it. It is shown that the CFL criteria successfully achieves during the simulation.

3. Theoretical analysis

The flow characteristics as well as the transportation of pollutants under such a scenario should be determined by the competition of buoyancy effect of the hot gases and the inertial effect of the wind flow. The buoyancy effect trends to promote the hazardous pollutant to rise and be exhausted from the top of the street canyon. At the same time, the inertial effect of the horizontal wind counteracts the buoyancy effect and tends to push the pollution plume to tilt at the top of the street canyon and force it come back to the street canyon. A dimensionless parameter, the local Froude number (Fr), which represents the ratio of the buoyancy force to the inertial force in the theory of turbulent buoyant flow dynamics, is introduced here to characterize the competition of the buoyant pollution plume flow ejected from the building with the inertial wind flow at the top of the street canyon. The Froude number is defined as [35]

$$\mathrm{Fr} = \frac{u}{\sqrt{(\Delta T_Z/T_a)gZ}} \tag{5}$$

where u is the wind velocity, ΔT_Z is the temperature differences between the gas flow and the ambient temperature, T_a is the ambient temperature, g is the acceleration of gravity and Z is the characteristic height, which is taken here as the height from the window to the top of the street canyon.

When the critical re-entrainment phenomenon occurs, the competition of the buoyancy force with the inertial force should achieve a balance and the Froude number should reach a certain constant critical value according to the flow dynamics theory. This indicates

$$u_c \propto (\Delta T_Z Z)^{1/2} \tag{6}$$

Yokoi [36] had correlated the dimensionless temperature of a window spill thermal plume based on experimental data and dimensional analysis. The dimensionless temperature Θ was defined as [36]

$$\Theta = \frac{\Delta T_Z r_0^{5/3}}{\sqrt[3]{\dot{Q}^2 T_a/{C_p}^2 {\rho_Z}^2 g}} \tag{7}$$

where r_0 is the equivalent radius of the heat source, $\dot{Q}$ is the convective buoyancy flow rate at the window, ρ_Z is the local density of the hot gases current and is usually taken as the value of the ambient air based on Boussinesq approximation for the buoyant plume. For the spill thermal plume away from the window exit at a height Z, the correlation of Yokoi [36] indicates

$$\Theta \propto \left(\frac{r_0}{Z}\right)^{5/3} \tag{8}$$

Substituting Eq. (7) into Eq. (8), being T_a, C_p, $\dot{Q}$ constants, it gives:

$$\Delta T_Z \propto Z^{-5/3} \tag{9}$$

And further substituting Eq. (9) into Eq. (6), it finally achieves

$$u_c \propto Z^{-1/3} \tag{10}$$

So, it is found that the critical re-entrainment wind velocity should be proportional to $-1/3$ power of the characteristic height.

4. Results and discussion

4.1. Smoke soot field and flow pattern

When there is a fire contamination source in the room, the hot dangerous smoke soot and gases will fill the room and then spill out from the window into the street canyon. The smoke soot fields for the case of fire contamination source positioned at the first floor are shown in Fig. 4, as well as to indicate the flow pattern under different wind velocities. It is worth mentioning that in the former work [23] dealing with a buoyancy source positioned at the center of the street canyon floor, four distinct regimes were identified to categorize the plume dispersion pattern characteristics under different levels of wind velocities. Under those situations, due to the wind-driven large vortex formed within the street canyon, the plume was found to curve along a circular route and finally be re-entrained back into the street canyon when the wind velocity was beyond a critical value [23]. However, when the plume was ejected from the adjacent building as the situation here, it was shown that the overall development of the flow can be characterized as a spill plume attaching to the wall before reaching the top of building, then along with an afterward tilted free plume being pushed downstream by the horizontal wind.

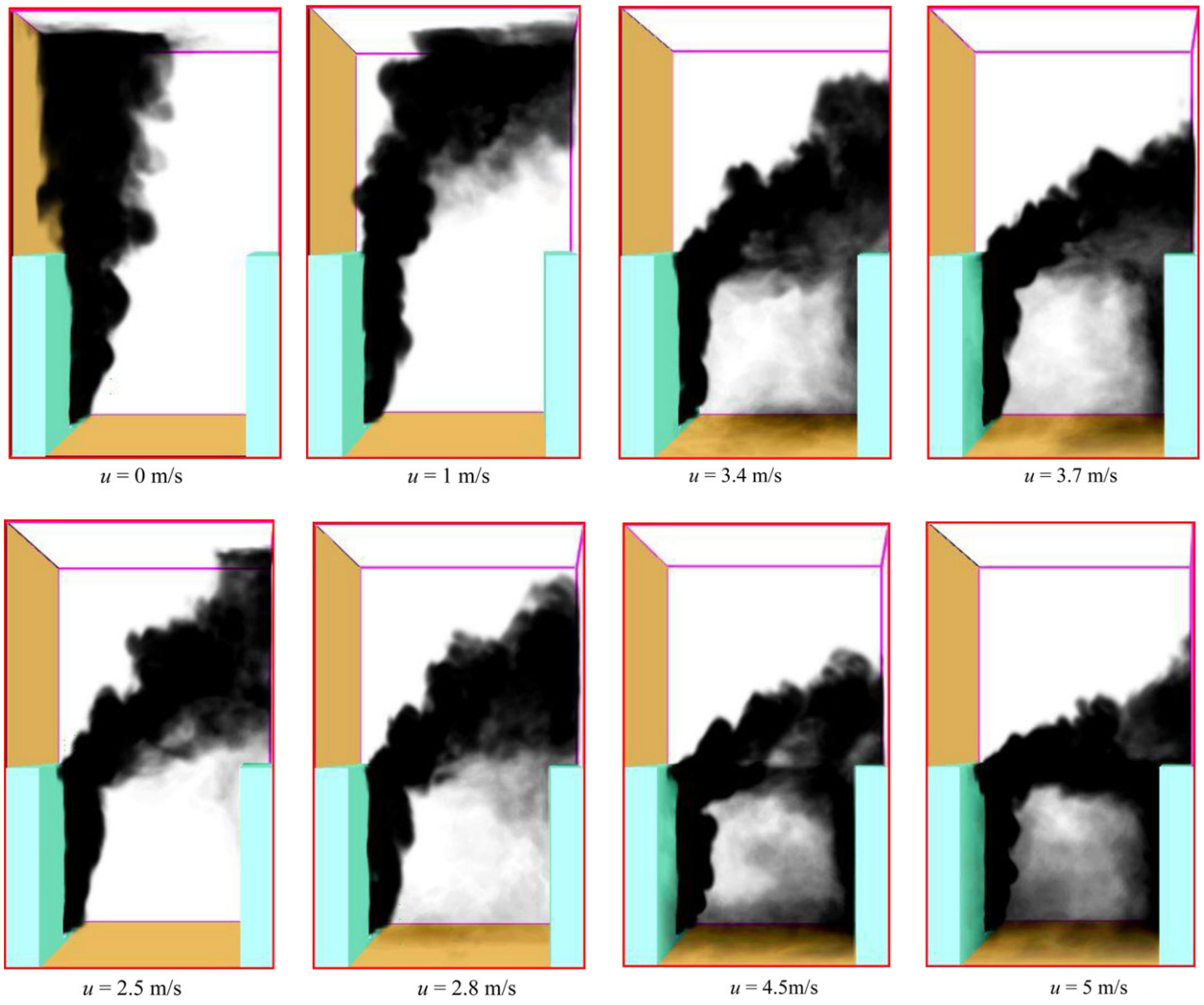

Fig. 4. Smoke soot field and flow pattern under different wind velocities.

When the wind velocity was relative small, for example, below 2.8 m/s in Fig. 4, the smoke spilled out of the burning room and then rose straight along the windward building of street canyon. When the smoke reached the top of street canyon, it was blown to the leeward building of street canyon by the wind, but still not touching the building in the leeward direction. When the wind velocity increased to be moderate, for example, between 2.8 m/s and 3.7 m/s in Fig. 4, the tilt angle of the plume above the top the building in the windward direction started to become considerably larger. At the same time, the lower edge of the contamination plume above the street canyon reached the leeward building. The critical re-entrainment velocity was determined based on the observation of the smoke flow behavior along the wall of the leeward building. With the increase in the wind velocity, the smoke plume finally begins to impinge on the wall of the leeward building. However, when the wind velocity is not high enough, the downward attaching-wall flow along the leeward building, which is counteracting the buoyancy of itself, cannot reach the floor level. The critical re-entrainment velocity was quantified as the wind velocity under which the downward attaching-wall smoke flow finally reaches the floor of the street canyon and then begins to go horizontally along the floor to the windward building. When the wind velocity exceeded this critical re-entrainment velocity, here as 2.8 m/s, the smoke soot was re-entrained into the street canyon. What was worse, the smoke was driven to the ground level and accumulated in the street canyon. It was really a very terrible situation because the visibility in atmosphere would be rather low, putting the vehicles and pedestrians in danger. And finally, when the wind velocity reached high levels, for example, larger than 3.7 m/s in Fig. 4, the smoke in the ground level in the leeward direction started to extend to the windward part of the street canyon. The entire street canyon was full of dangerous smoke. So, once the wind velocity exceeded the critical re-entrainment velocity, the smoke was re-entrained back into street canyon and the vehicles and pedestrians would be in great danger. The critical re-entrainment velocity should be studied as an important parameter.

4.2. Temperature and CO concentration contours

The temperature above ambient is the source contribution to the buoyancy force. The temperature contours in and above the street canyon for buoyancy sources positioned at different floors with wind velocity of 1 m/s are shown in Fig. 5. The temperature was shown to become lower and lower when rising up. At the bottom of the plume, the temperature was high. Considering the buoyant contamination source at different floors, it was shown that when the fire or explosion occurred at higher floors, the gas temperature the top of the street canyon was higher. So, it was indicated that higher wind velocity was needed to re-entrain the pollutant

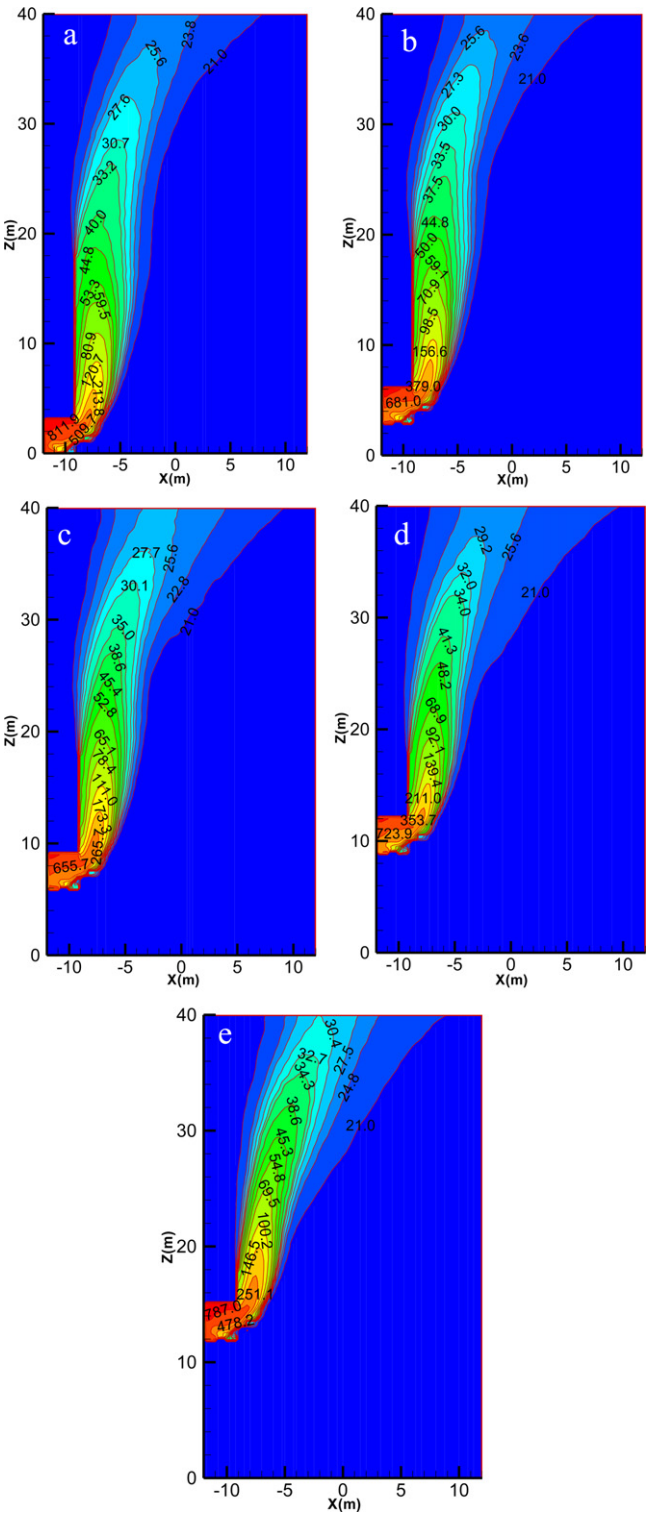

Fig. 5. Temperature contour with buoyant contamination source at different floors (u = 1 m/s).

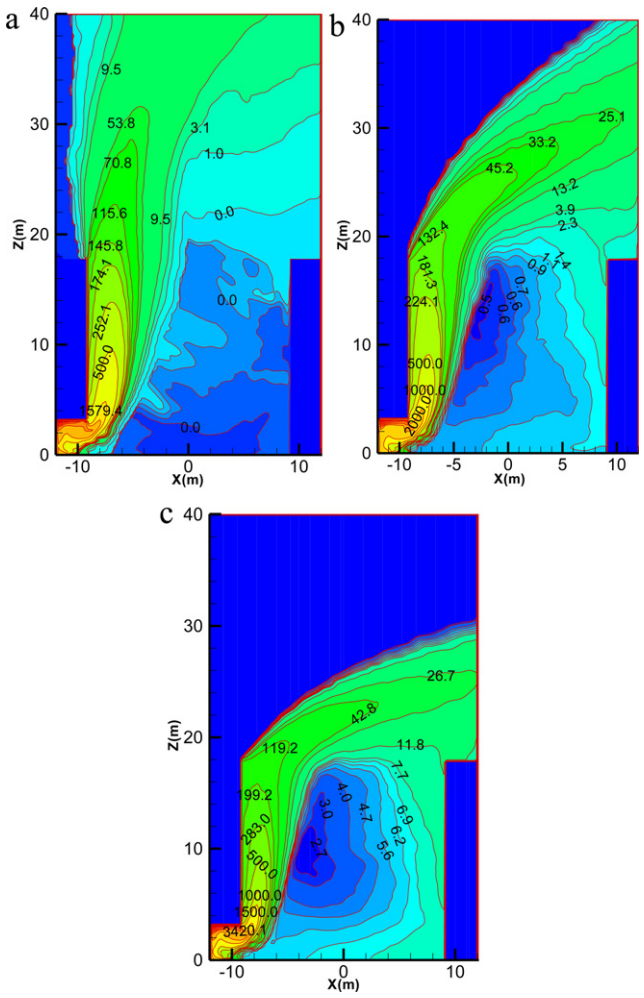

Fig. 6. CO concentration contours under different wind velocities.

gas back into the street canyon when the buoyancy source was positioned at higher floors.

Fig. 6 presents the CO concentration contours in and above the street canyon under different wind velocities. It was shown that the CO concentration distribution for the pollutant plume was similar to that of the temperature, which became lower and lower with height. And it was obvious that the CO concentration in the plume region was higher than that at the other part of the street canyon. In addition, from Fig. 6, it was found that with the increase in the wind velocity, the CO distribution in the plume region remained basically unchanged, which indicated that the influence of the wind velocity on the CO concentration in the plume region was negligible.

Fig. 6(a) shows the CO concentration contours with wind velocity of 1 m/s. It was found that when the wind velocity was relative small, the CO concentration contour shape outside the plume regime was very irregular and the CO concentration value there was very low. This was because the weak wind cannot effectively counteract and scatter the buoyant plume. When the critical re-entrainment wind velocity, 2.8 m/s, was reached, the concentration of CO outside the plume regime was becoming much greater. This was explained by the entrainment of the hot smoke and gas back into the canyon. A characteristic large vortex was shown for the CO concentration contour shape. However, for wind velocity of 5 m/s, the large vortex became more obvious and regular. The concentration of CO outside the plume region showed a higher level than the other two cases. It can be explained by the fact that with the increase in wind velocity, more and more smoke was re-entrained back into the street canyon.

4.3. Correlating critical re-entrainment velocity with characteristic height

As the ratio of inertial forces to buoyancy force, Froude number is a very important parameter. The Froude number values of the plume when reaching the top of the street canyon under different

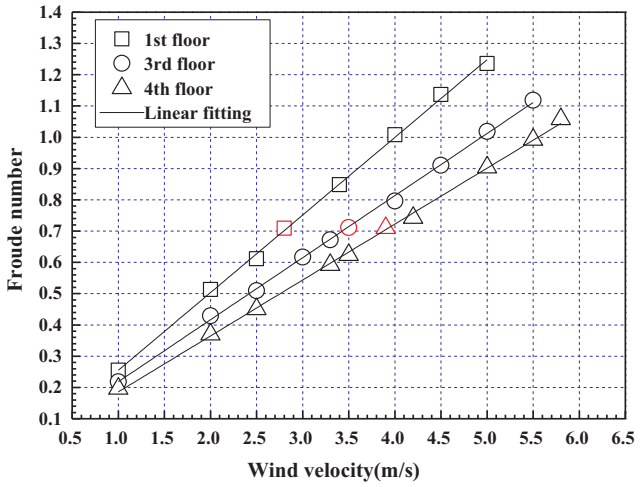

Fig. 7. Variation of Froude numbers with wind velocities for buoyant contamination source at different floor.

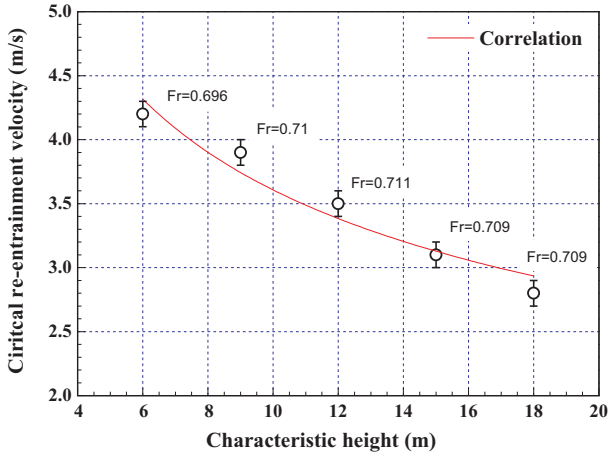

Fig. 8. Critical re-entrainment wind velocity vs. characteristic height.

wind velocities are presented in Fig. 7. It was shown that with the increase in the wind velocity, the Froude number became higher. They had a good positively linear relationship, as in accordance with Eq. (5). The Froude number was larger when the buoyancy source was positioned at lower floors, as the corresponding pollution temperature at the top of the street canyon was lower. However, when the critical re-entrainment wind velocity was achieved, the Froude number values were all shown to be near to 0.7, regardless of floor height of the source room, as marked by red colour in Fig. 7. (For interpretation of the references to colour in this figure, the reader is referred to the web version of this article.) This finding was of great significance, which meant that the ratio of inertial force of the wind flow to the buoyancy force of the pollution plume flow was a constant value when the critical re-entrainment phenomenon was coming forth. When the Froude number exceeded this critical re-entrainment Froude number, the dangerous gas would be re-entrained back into street canyon.

Fig. 8 correlates the critical re-entrainment wind velocity against the characteristic height based on the LES simulation results. It was shown that their relationship can be well approached by a power law function of $y = ax^b$. The correlation coefficient was 0.9631. Correlating result for the power index of Z was −0.351, which was very close to the theoretical value of −1/3. The LES simulation result agreed well with the theoretical analysis.

5. Conclusion

The buoyancy effect on the dispersion characteristics of smoke soot and CO gas ejected from the adjacent building into an urban street canyon under a perpendicular wind flow was investigated by fire dynamics simulator (FDS), large eddy simulation (LES). Theoretical analysis was also performed to consider the relationship between the critical re-entrainment wind velocity and the characteristic height. Results showed that the flow pattern in and above the street canyon can be characterized as a spill plume attaching to the wall before reaching the top of building and afterward a tilted free plume being pushed downstream by the horizontal wind. The CO dispersion and the consequent concentration pattern in the plume region within the street canyon are slightly sensitive to the wind velocity. On the other hand, results have shown that the dispersion is strongly affected by the wind velocity in other regions inside the street canyon. A regular characteristic large vortex was shown for the CO concentration contour shape when the wind velocity was higher than the critical re-entrainment value. The values of Froude number at the top of the street canyon were found to vary proportionally with the wind velocity. The critical Froude number corresponding to the critical re-entrainment phenomenon was found to be a constant value of 0.7. The critical re-entrainment wind velocities, u_c, for buoyant contamination source at different floors of the building, was proportional to −1/3 power of the characteristic height from the fire floor to the top of the street canyon. LES simulation result agreed well with the theoretical analysis.

Acknowledgement

This article was supported by Nature Foundation of China under Grant No.40975005, Fundamental Research Funds for the Central Universities, and Program for New Century Excellent Talents in University under Grant No. NCET-09-0914.

References

[1] S. Vardoulakis, B.E.A. Fisher, K. Pericleous, N. Gonzalez-Flesca, Modelling air quality in street canyons: a review, Atmos. Environ. 37 (2003) 155–182.
[2] M.W. Rotach, Profiles of turbulence statistics in and above an urban street canyon, Atmos. Environ. 29 (1995) 1473–1486.
[3] N.A. Mazzeo, L.E. Venegas, P.B. Martin, Analysis of full-scale data obtained in a street canyon, Atmosfera 20 (2007) 93–110.
[4] S. Xie, Y. Zhang, L. Qi, X. Tang, Spatial distribution of traffic-related pollutant concentrations in street canyons, Atmos. Environ. 37 (2003) 3213–3224.
[5] I. Eliasson, B. Offerle, C.S.B. Grimmond, S. Lindgvist, Wind fields and turbulence statistic in an urban street canyon, Atmos. Environ. 40 (2006) 1–16.
[6] R.N. Meroney, M. Pavageau, S. Rafailidis, M. Schatzmann, Study of line source characteristics for 2-D physical modeling of pollutant dispersion in street canyons, J. Wind Eng. Ind. Aerod. 62 (1996) 37–56.
[7] P. Kastner-Klein, E.J. Plate, Wind-tunnel study of concentration fields in street canyons, Atmos. Environ. 33 (1999) 3973–3979.
[8] K. Uehara, S. Murakami, S. Oikawa, S. Wakamatsu, Wind tunnel experiments on how thermal stratification affects flow in and above urban street canyons, Atmos. Environ. 34 (2000) 1553–1562.
[9] M. Pavageau, M. Schatzmann, Wind tunnel measurements of concentration fluctuations in an urban street canyon, Atmos. Environ. 33 (1999) 3961–3971.
[10] X.X. Li, D.Y.C. Leung, C.H. Liu, Physical modeling of flow field inside urban street canyons, J. Appl. Meteorol. Climate 47 (2008) 2058–2067.
[11] H.Z. Liu, B. Liang, F.R. Zhu, B.Y. Zhang, J.G. Sang, A laboratory model of the flow in urban street canyons induced by bottom heating, Adv. Atmos. Sci. 20 (2003) 554–564.
[12] V.D. Assimakopoulos, H.M. ApSimon, N. Moussiopoulos, A numerical study of atmospheric pollutant dispersion in different two-dimensional street canyon configurations, Atmos. Environ 37 (2003) 4037–4049.
[13] Z.T. Xie, I.P. Castro, Large-eddy simulation for flow and dispersion in urban streets, Atmos. Environ. 43 (2009) 2174–2185.
[14] R. Yang, J. Zhang, S.F. Shen, X.M. Li, J.G. Chen, Numerical investigation of the impact of different configurations and aspect ratios on dense gas dispersion in urban street canyons, Tsinghua Sci. Technol. 12 (3 June) (2007) 345–351, ISSN: 1007-0214 17/18.
[15] J. Baker, H.L. Walker, X.M. Cai, A study of the dispersion and transport of reactive pollutants in and above street canyons—a large eddy simulation, Atmos. Environ. 38 (2004) 6883–6892.

[16] J.J. Kim, J.J. Baik, Urban street-canyon flows with bottom heating, Atmos. Environ. 35 (20) (2001) 3395–3404.
[17] J.J. Kim, J.J. Baik, Effects of street-bottom and building-roof heating on flow in three-dimensional street canyons, Adv. Atmos. Sci. 27 (3) (2010) 513–527.
[18] A.K. Panskus, L. Moulinneuf, E. Savory, A. Abdelquari, J.F. Sini, J.M. Rosant, A. Robins, N. Toy, A wind tunnel investigation of the influence of solar-induced wall heating on the flow regime within a simulated urban street canyon, J. Water, Air, Soil Pollut.: Focus 2 (2002) 555–571.
[19] K. Richards, M. Schatzmann, B. Leitl, Wind tunnel experiments modelling the thermal effects within the vicinity of a single block building with leeward wall heating, J. Wind Eng. Ind. Aerod. 94 (2006) 621–636.
[20] R. Dimitrova, J.F. Sini, K. Richards, M. Schatzmann, M. Weeks, E. Perez García, C. Borrego, Influence of thermal effects on the wind field within the urban environment, Bound.-Layer Meteorol. 131 (2009) 223–243.
[21] J. Ovadnevaite, K. Kvietkus, A. Marsalka, 2002 summer fires in Lithuania: impact on the Vilnius city air quality and the inhabitants health, Sci. Total Environ. 356 (2006) 11–21.
[22] R. Besserre, P. Delort, Recent studies prove that the main cause of death during urban fires is poisoning by smoke, Urgences Medicales 16 (1997) 77–80.
[23] L.H. Hu, R. Huo, D. Yang, Large eddy simulation of fire-induced buoyancy driven plume dispersion in an urban street canyon under perpendicular wind flow, J. Hazard. Mater. 166 (2009) 394–406.
[24] L.H. Hu, W. Peng, R. Huo, Critical wind velocity for arresting upwind gas and smoke dispersion induced by near-wall fire in a road tunnel, J. Hazard. Mater. 150 (2008) 68–75.
[25] Y. Tominaga, A. Mochida, R. Yoshie, H. Kataoka, T. Nozu, M. Yoshikawa, T. Shirasawa, AIJ guidelines for practical applications of CFD to pedestrian wind environment around buildings, J. Wind Eng. Ind. Aerod. 96 (2008) 1749–1761.
[26] K.B. McGrattan, Randall McDermott, S. Hostikka, J.E. Floyd. Fire Dynamics Simulator (Version 5), User's Guide. NIST Special Publication 1019-5, National Institute of Standards and Technology, Gaithersburg, Maryland, October 2010.
[27] K.B. McGrattan, S. Hostikka, J.E. Floyd, H.R. Baum, R.G. Rehm, W.E. Mell, R. McDermott. Fire Dynamics Simulator (Version 5), Technical Reference Guide, Volume 1: Mathematical Model. NIST Special Publication 1018-5, National Institute of Standards and Technology, Gaithersburg, Maryland, October 2010.
[28] C.-H. Chang, Computational fluid dynamics simulation of concentration distributions from a point source in the urban street canyons, J. Aerospace Eng. 19 (2) (2006) 80–86.
[29] W. Zhang, A. Hamer, M. Klassen, D. Carpenter, R. Roby, Turbulence statistics in a fire room model by large eddy simulation, Fire Safety J. 37 (2002) 721–752.
[30] P.D. Lax, Hyperbolic difference equations: a review of the Courant–Friedrichs–Lewy paper in light of recent developments, IBM J. Res. Dev. 11 (1967) 235–238.
[31] P. Salizzoni, N. Grosjean, P. Mejean, R.J. Perkins, L. Soulhac, R. Vanliefferinge, Wind tunnel study of the exchange between a street canyon and the external flow, Air Pollut. Model.Appl. XVII (2007) 430–437.
[32] L.H. Hu, N.K. Fong, L.Z. Yang, W.K. Chow, Y.Z. Li, R. Huo, Modeling fire-induced smoke spread and carbon monoxide transportation in a long channel: fire dynamics simulator comparisons with measured data, J. Hazard. Mater. 140 (2007) 293–298.
[33] L.H. Hu, R. Huo, W. Peng, W.K. Chow, R.X. Yang, On the maximum smoke temperature under ceiling in tunnel fires, Tunn. Underground Space Technol. 21 (2006) 650–655.
[34] L.H. Hu, R. Huo, W.K. Chow, Studies on buoyancy-driven back-layering in tunnel fires, Exp. Therm. Fluid Sci. 32 (2008) 1468–1483.
[35] Y. Oka, O. Sugawa, T. Imamura, Correlation of temperature rise and velocity along an inclined fire plume axis in crosswinds, Fire Saf. J. 43 (2008) 391–400.
[36] S. Yokoi, Study on the prevention of fire spread caused by hot upward current, Japanese Ministry of Construction, Building Research Institute Report 34 1960.